MODULE-II- Basic Aerodynamics

Overview

The primary forces that act on an air vehicle are thrust, lift, drag, and gravity (or weight). They are shown in Figure 3.1. In addition, angular moments about the pitch, roll, and yaw axes cause the vehicle to rotate about those axes. Lift, drag, and rotational moments are computed from dynamic pressure, wing area, and dimensionless co-efficients. The expressions for these quantities are the fundamental aerodynamic equations that govern the performance of an air vehicle.

Basic Aerodynamic Equations

The dynamic pressure, q, of a moving airstream is given by:

$$q = \frac{1}{2}\rho V^2 \qquad (1)$$

where ρ is air density and V is velocity. The forces acting on an airplane wing are a function of q, the wing area S, and dimensionless co-efficients (C_l, C_d, and C_m) that depend on Reynolds number, Mach number, and the shape of the cross-section of the wing. The first two forces, lift and drag, are written as follows:

$$L = C_l qS \qquad (2)$$

$$D = C_d qS \qquad (3)$$

The third force of this aerodynamic triumvirate is pitching moment, which must include an additional term to dimensionally create a moment. The wing chord, c (see Figure 3.2), is the usual distance chosen as the moment arm. Knowledge of the pitching moment is critical to the understanding of stability and control:

$$M = C_m qSc \qquad (4)$$

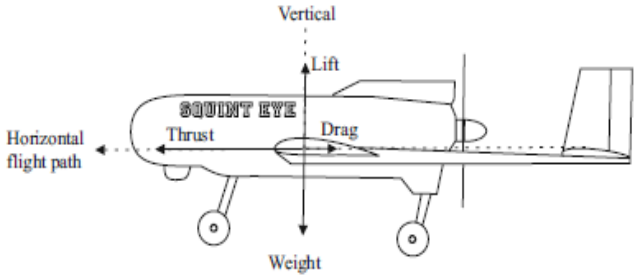

Figure 3.1 Forces on air vehicle

C_l, C_d, and C_m characterize the lift, drag, and moment for any airfoil cross-section, and are the aerodynamic coefficients of primary interest to the UAV designer. There are other coefficients, called stability derivatives, but they are specialized functions that influence the dynamic characteristics of the air vehicle and their discussion is beyond the scope of this text. Any particular airfoil cross-sectional shape has a characteristic set of curves for the coeffi- cients of lift, drag, and moment that depend on angle of attack and Reynolds number. These are determined from wind tunnel tests and are designated by lowercase subscripts. Figure 3.2 shows the geometry of an airfoil section and the directions of lift and drag. Lift is always perpendicular and drag always parallel to the relative wind. The moment can be taken with respect to any point, but traditionally is taken about a point 25% rearward of the wing leading edge known as the quarter chord.

Basic aerodynamic data are usually measured from a wing that extends from wall to wall in the wind tunnel as shown in Figure 3.3. Extending the wing from wall to wall prevents spanwise airflow and results in a true two-dimensional pattern of air pressure. This concept is called the infinite-span wing because a wing with an infinite span could not have air flowing around its tips, creating spanwise flow and disturbing the two-dimensional pressure pattern that is a necessary starting point for describing the aerodynamic forces on a wing. A real airplane wing has a finite span, and perhaps taper and twist, but the analysis of aerodynamic forces begins with the two-dimensional coefficients, which then are adjusted to account for the three-dimensional nature of the real wing.

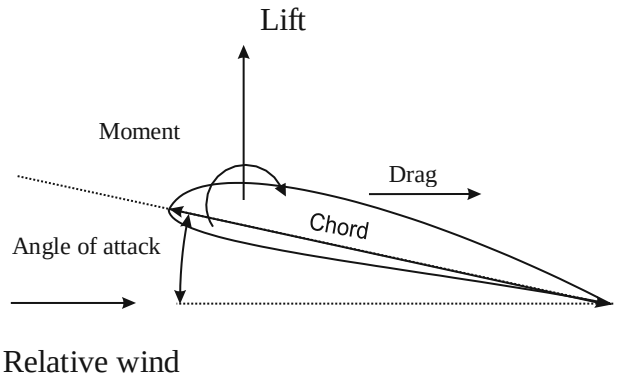

Figure 3.2 Airfoil geometry

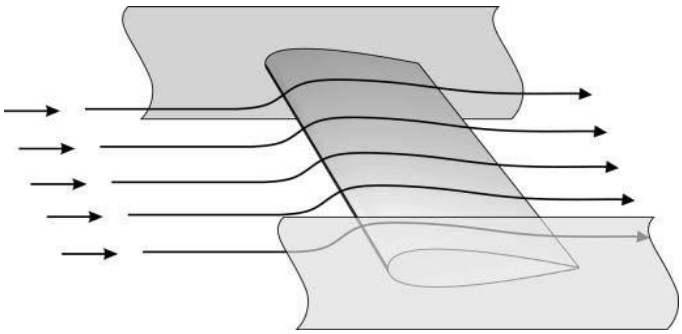

Figure 3.3 Infinite span wing

Airfoil cross-sections and their two-dimensional coefficients are classified in a standard system maintained by the National Aeronautics and Space Administration (NASA) and identified by a NASA numbering system. Figures 3.4–3.6 show the data contained in the summary charts of the NASA database for NASA airfoil 23201 as an example of the information available on many airfoil designs. Figure 3.4 shows the profile of a cross-section of the airfoil. The x (horizontal) and y (vertical) coordinates of the surface are plotted as x/c and y/c, where c is the chord of the airfoil, its total length from nose to tail. Two-dimensional lift and moment coefficients for this airfoil are plotted as a function of angle of attack in Figure 3.5.

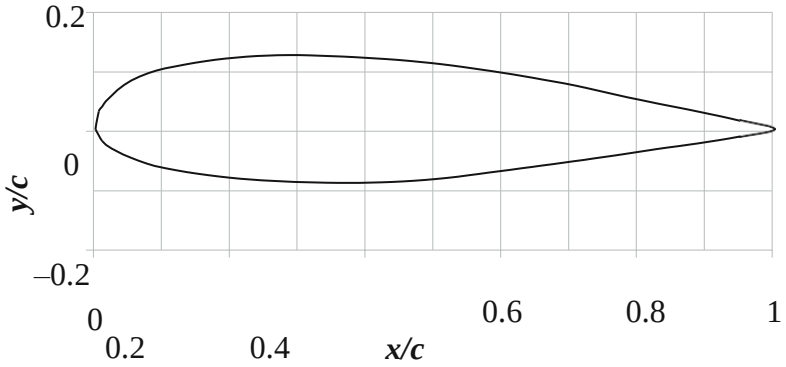

Figure 3.4 NASA 23021 airfoil profile

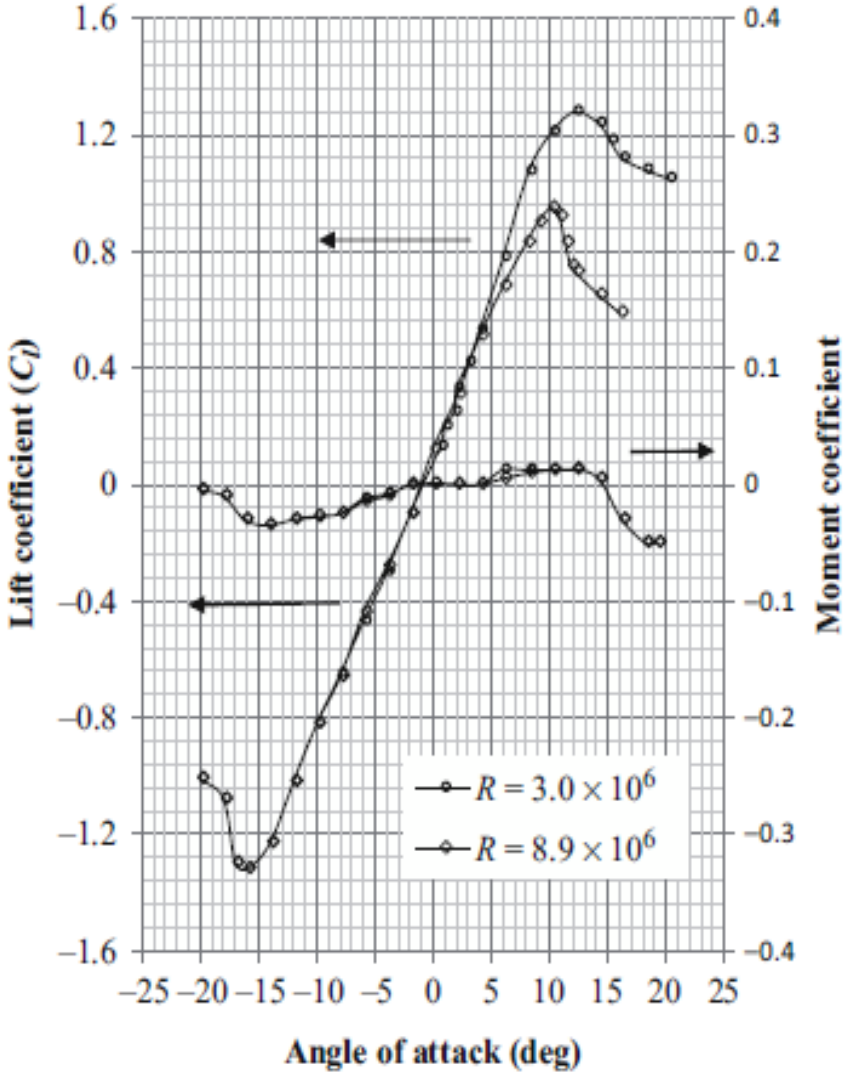

The moment coefficient in the plot is around an axis located at the quarter-cord, as mentioned previously. Figure 3.5 shows two curves for each co-efficient. Each curve is for a specified Reynolds number. The NASA database contains data for more than two Reynolds numbers, but Figure 3.5 reproduces only $R = 3.0 * 10^6$ and $R = 8.9*10^6$. The two moment curves lie nearly on top of each other and cannot be distinguished. Figure 3.6 shows the two-dimensional drag coefficient and the moment coefficient as a function of the lift co-efficient.

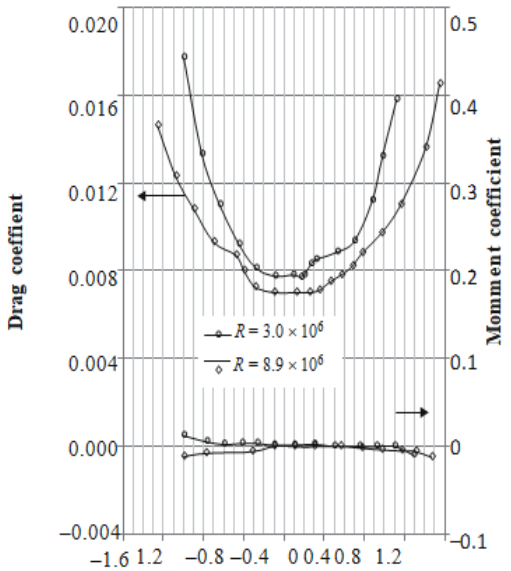

Aircraft Polar

Aircraft or drag "polar," a term introduced by Eiffel years ago, which is a curve of C_L plotted against C_D. A typical airplane polar curve is shown in Figure 3.7. The drag polar will later be shown to be parabolic in shape and define the minimum drag, C_{D0}, or drag that is not attributable to the generation of lift. A line drawn from the origin and tangent to the polar gives the minimum lift-to-drag ratio that can be obtained. It will also be shown later that the reciprocal of this ratio is the tangent of the power-off glide angle of an air vehicle. The drag created by lift or induced drag is also indicated on the drag polar.

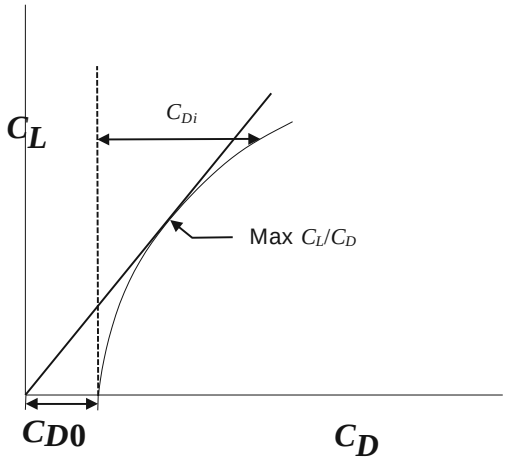

Figure 3.7 Aircraft polar

The Real Wing and Airplane

A real three-dimensional aircraft normally is composed of a wing, a fuselage, and a tail. The wing geometry has a shape, looking at it from the top, called the planform. It often has twist, sweepback, and dihedral (angle with the horizontal looking at it from the front) and is composed of two-dimensional airfoil sections. A full analysis for lift and drag must consider not only the contribution of the wing but also by the tail and fuselage and must account for varying airfoil cross-section characteristics and twist along the span.

Determining the three-dimensional moment coefficient also is a complex procedure that must

take into account, the contributions from all parts of the aircraft. Figure 3.8 is a simplified moment balance diagram of the aerodynamic forces acting on the aircraft. Summing these forces about the aircraft center of gravity (CG) results in Equation (3.6):

$$M_{CG} = Lx_a + Dz_a + m_{ac} - L_t x_t + m_{act} (\text{if } D_t = 0) \qquad (3.6)$$

where m_{ac} and m_{act} are the separate pitching moments of the wing and tail.

Dividing by q/Sc (see Equation (3.4)), the three-dimensional pitching moment coefficient about the CG is obtained as shown in Equation (3.7), where S_t is the area of the tail surface and S the area of the wing. Pitching moment, the torque about the aircraft center of gravity, has a profound effect on the pitch stability of the air vehicle. A negative pitching moment coefficient is required to maintain stability and is obtained primarily from the tail (the last two terms in the equation):

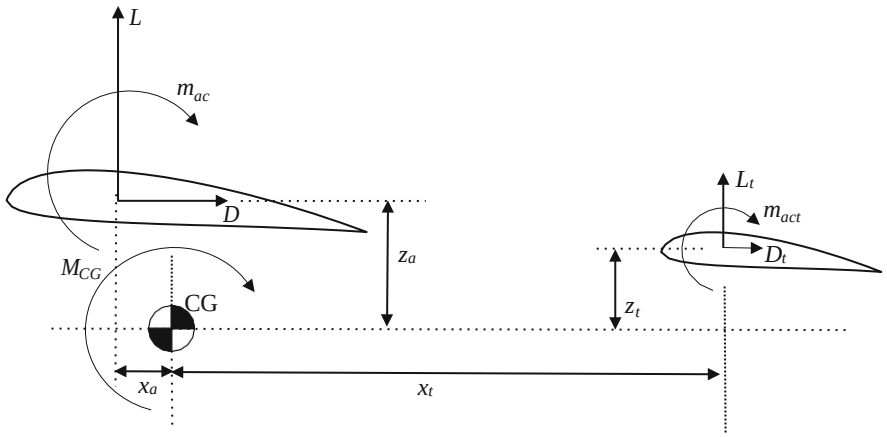

Figure 3.8 Moment balance diagram

has a profound effect on the pitch stability of the air vehicle. A negative pitching moment coefficient is required to maintain stability and is obtained primarily from the tail (the last two terms in the equation):

$$C_{M_{CG}} = C_L\left(\frac{x_a}{c}\right) + C_D\left(\frac{z_a}{c}\right) + C_{m_{ac}} + C_{fus} - C_{L_t}\left(\frac{S_t}{S}\right)\left(\frac{x_t}{c}\right) + C_{m_{act}} \qquad (3.7)$$

A crude estimate (given without proof) of the three-dimensional wing lift coefficient, indicated by an uppercase subscript, in terms of the "infinite wing" coefficient is:

$$C_L = \frac{C_l}{\left(1 + \frac{2}{AR}\right)} \qquad (3.8)$$

where AR is the aspect ratio (wingspan squared divided by wing area) or b^2/S.

From this point onward, we will use uppercase subscripts and assume that we are using coefficients that apply to the real wing and aircraft.

Induced Drag

Drag of the three-dimensional airplane wing plays a particularly important role in airplane design because of the influence of drag on performance and its relationship to the size and shape of the wing planform. The most important element of drag introduced by a wing is the "induced drag," which is drag that is inseparably related to the lift provided by the wing. Consider the pressure distribution about an airfoil as shown in Figure 3.9. It is apparent that a wing would have positive pressure on its underside and negative (in a relative sense) pressure on the top. This is shown in Figure 3.10 as plus signs on the bottom and minus signs on the top as viewed from the front or leading edge of the wing. Such a condition would allow air to spill over from the higher pressure on the bottom surface to the lower pressure top causing it to swirl or form a vortex. The downward velocity or downwash onto the top of the wing created by the swirl would be greatest at the tips and reduced toward the wing center as shown in Figure 3.11.

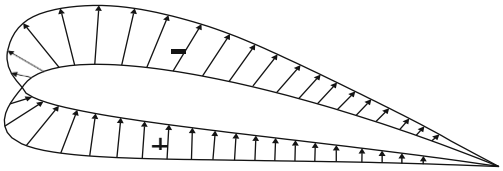

Figure 3.9 Pressure Distribution

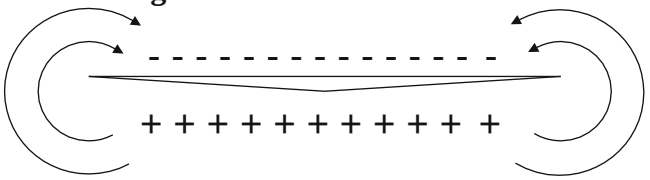

Figure 3.10 Spanwise pressure distribution

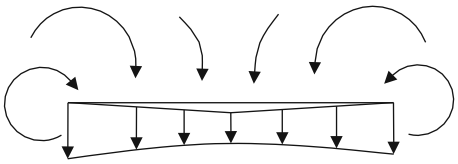

Downwash (w)

Figure 3.11 Downwash

Ludwig Prandtl has shown that a wing whose planform is elliptical would have an elliptical lift distribution and a constant downwash along the span, as shown in Figure 3.12. The notion of a constant downwash velocity (w) along the span will be the starting point for the development of the effect of three-dimensional drag. Considering the geometry of the flow with downwash as shown in Figure 3.13, it can be seen that the downward velocity component for the airflow over the wing (w) results in a local "relative wind" flow that is deflected downward. This is shown at the bottom, where w is added to the velocity of the air mass passing over the wing (V) to determine the effective local relative wind (V_{eff}) over the wing. Therefore, the wing "sees" an angle of attack that is less than it would have had there been no downwash. The lift (L) is perpendicular to V and the net force on the wing is perpendicular to V_{eff}. The difference between these two vectors, which is parallel to the velocity of the wing through the air mass, but opposed to it in direction, is the induced drag (D_i).

This reduction in the angle of attack is:

$$\varepsilon = \tan^{-1}\left(\frac{w}{V}\right) \qquad (3.9)$$

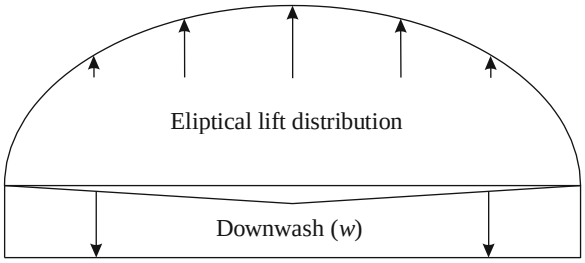

Figure 3.12 Elliptical lift distribution

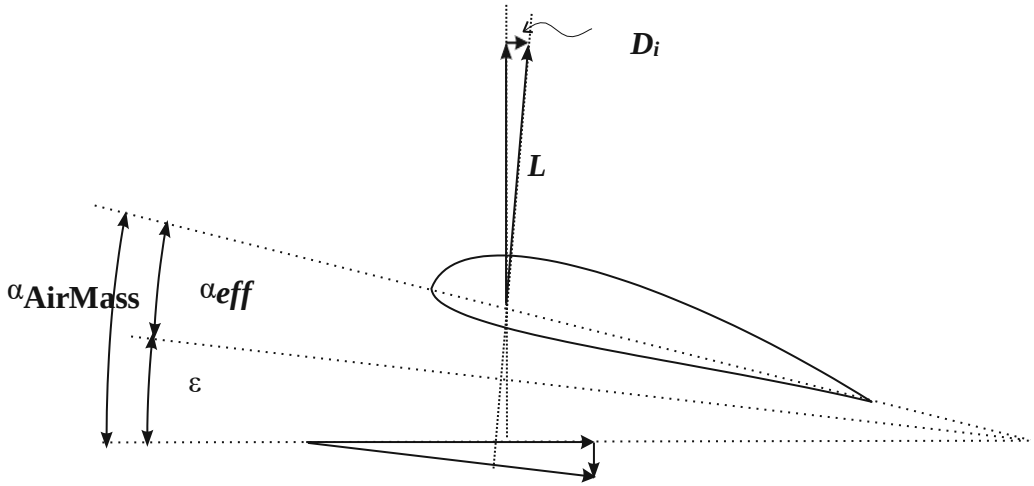

Figure 3.13 Induced drag diagram

From Figure 3.13, one can see that the velocity and force triangles are similar, so:

$$\frac{D_i}{L} = \frac{w}{V}$$

Dividing by q (see Equations (3.1) through (3.3)):

$$\frac{C_{Di}}{C_L} = \frac{w}{V}$$

For the case of an elliptical lift distribution, Ludwig Prandtl has shown that:

$$\frac{w}{V} = \frac{C_L}{\pi AR}$$

then the induced drag coefficient (C_{Di}) is given by:

$$C_{Di} = \frac{C_L^2}{\pi AR} \qquad (3.10)$$

This expression reveals to us that air vehicles with short stubby wings (small *AR*) will have relatively high-induced drag and therefore suffer in range and endurance. Air vehicles that are required to stay aloft for long periods of time and/or have limited power, as, for instance, most electric-motor-driven UAVs, will have long thin wings.

The Boundary Layer

A fundamental axiom of fluid dynamics is the notion that a fluid flowing over a surface has a very thin layer adjacent to the surface that sticks to it and therefore has a zero velocity. The next layer (or lamina) adjacent to the first has a very small velocity differential, relative to the first layer, whose magnitude depends on the viscosity of the fluid. The more viscous the fluid, the lower the velocity differential between each succeeding layer. At some distance δ, measured

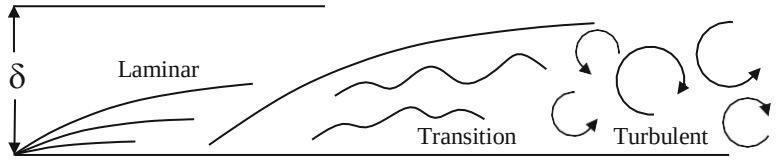

Figure 3.14 Typical boundary layer

perpendicular to the surface, the velocity is equal to the free-stream velocity of the fluid. The distance δ is defined as the thickness of the boundary layer. The boundary is composed of three regions beginning at the leading edge of a surface: (1) the laminar region where each layer or lamina slips over the adjacent layer in an orderly manner creating a well-defined shear force in the fluid, (2) a transition region, and (3) a turbulent region where the particles of fluid mix with each other in a random way creating turbulence and eddies. The transition region is where the laminar region begins to become turbulent. The shear force in the laminar region and the swirls and eddies in the turbulent region both create drag, but with different physical processes. The cross-section of a typical boundary layer might look like Figure 3.14.

The shearing stress that the fluid exerts on the surface is called skin friction and is an important component of the overall drag. The two distinct regions in the boundary layer (laminar and turbulent) depend on the velocity of the fluid, the surface roughness, the fluid density, and the fluid viscosity. These factors explained by the Reynolds number, which mathematically is expressed as:

$$R = \rho V \frac{l}{\mu} \qquad (3.11)$$

where ρ is fluid density, V is fluid velocity, μ is fluid viscosity, and l is a characteristic length. In aeronautical work, the characteristic length is usually taken as the chord of a wing or tail surface. The Reynolds number is an important indicator of whether the boundary layer is in a laminar or turbulent condition. Laminar flow creates considerably less drag than turbulent but nevertheless causes difficulties with small surfaces. Typical Reynolds numbers are:

General Aviation Aircraft	**5,000,000**
Small UAVs	**400,000**
A Seagull	**100,000**
A Gliding Butterfly	**7,000**

Laminar flow causes drag by virtue of the friction between layers and is particularly sensitive to the surface condition. Normally, laminar flow results in less drag and is desirable. The drag of the turbulent boundary layer is caused by a completely different mechanism that depends on knowledge of Bernoulli's theorem. Bernoulli has shown that for an ideal fluid (no friction) the sum of the static pressure (P) and the dynamic pressure (q),

where. (3.12)

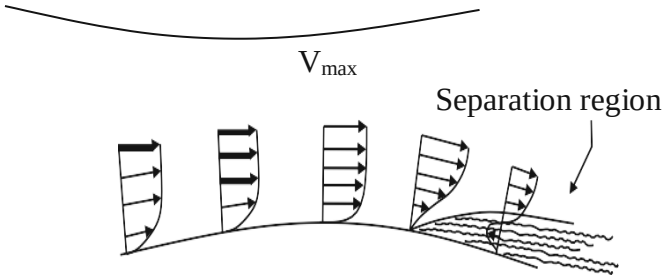

Figure 3.15 Boundary layer velocity profile

Applying this principle to flow in a venturi, with the bottom half representing an airplane wing, the distribution of pressure and velocity in a boundary layer can be analyzed. As the fluid (assumed to be incompressible) moves through the venturi or over a wing, its velocity increases (because of the law of conservation of mass) and, as a consequence of Bernoulli's theorem, its pressure decreases, causing what is known as a favorable pressure gradient. The pressure gradient is favorable because it helps push the fluid in the boundary layer on its way. After reaching a maximum velocity, the fluid begins to slow and consequently forms an unfavorable pressure gradient (i.e., hinders the boundary layer flow) as seen by the velocityprofiles in Figure 3.15.

Small characteristic lengths and low speeds result in low Reynolds numbers and conse- quently laminar flow, which is normally a favorable condition. A point is reached in this situation where the unfavorable pressure gradient actually stops the flow within the boundary layer and eventually reverses it. The flow stoppage and reversal results in the formation of turbulence, vortices, and in general a random mixing of the fluid particles. At this point, the boundary layer detaches or separates from the surface and creates a turbulent wake. This phenomenon is called separation, and the drag associated with it is called pressure drag. The sum of the pressure drag and skin friction (friction drag—primarily due to laminar flow) on a wing is called profile drag. This drag exists solely because of the viscosity of the fluid and the boundary layer phenomena.

Whether the boundary layer is turbulent or laminar depends on the Reynolds number, as does the friction coefficient, as shown in Figure 3.16.

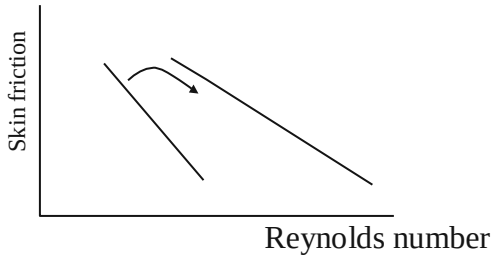

Figure 3.16 Skin friction versus Reynolds number

It would seem that laminar flow is always desired (for less pressure drag), and usually it is, but it can become a problem when dealing with very small UAVs that fly at low speeds. Small characteristic lengths and low speeds result in low Reynolds numbers and consequently laminar flow, which is normally a favorable condition. The favorable and unfavorable pressure gradients previously described also exist at very low speeds, making it possible for the laminar boundary layer to separate and re attach itself. This keeps the surface essentially in the laminar flow region, but creates a bubble of fluid within the boundary layer. This is called laminar separation and is a characteristic of the wings of very-small, low-speed airplanes (e.g. small model airplanes and very small UAVs).

Flapping Wings

There is interest in UAVs that use flapping wings to fly like a bird, the basic aerodynamics can be appreciated based on the same mechanisms for generating aerodynamic forces that we have outlined for fixed wings. The flapping of the wings of birds is not a pure up and down or rowing backstroke as commonly thought. The wings of a flying bird move up and down as they are flapped, but they also move

forward due to the bird's velocity through the air mass. Figure 3.17 shows the resulting velocity and force triangles when the wing is moving downward.

The net velocity of the wing through the air mass is the sum of the forward velocity of the bird's body (*V*) and the downward velocity of the wing, driven by the muscles of the bird (*w*), which varies over the length of the wing, being greatest at the wing tip. The resulting total velocity through the air mass is forward and down, which means that the relative wind over the wing is to the rear and up. The net aerodynamic force generated by that relative wind (*F*) is perpendicular to the relative wind and can be resolved into two components, lift (*L*) upward and thrust (*T*) forward.

The velocity and force triangles vary along the length of the wing because *w* is approximately zero at the root of the wing, where it joins the body of the bird and has a maximum value at the tip of the wing, so that the net force, *F*, is nearly vertical at the root of the wing and tilted furthest forward at the tip. As a result, it sometimes is said that the root of the bird's wing produces mostly lift and the tip produces mostly thrust. It is also possible for the bird to introduce a variable twist in the wing over its length, which could maintain the same angle of attack as *w* increases and the relative wind becomes tilted more upward near the tip. This twist can also be used to create an optimum angle of attack that varies over the length of the wing. This can be used to increase the thrust available from the wing tip. Figure 3.18 shows how flapping the wing up and down can provide net lift and net positive thrust.

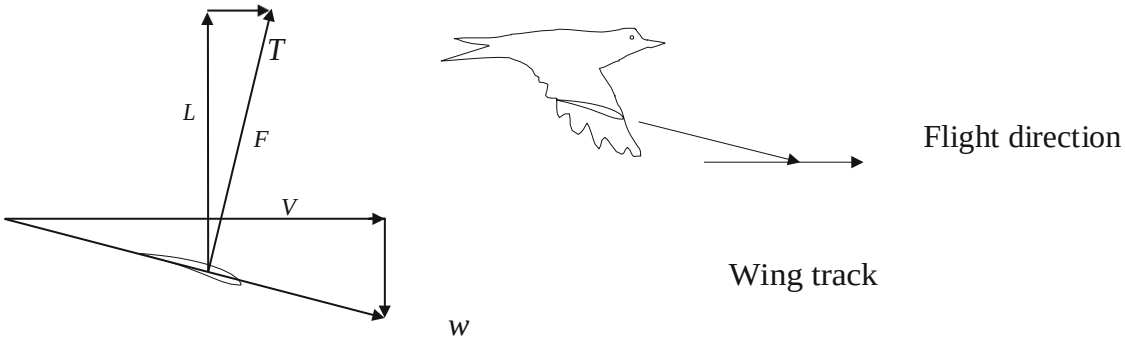

Figure 3.17 Wing flapping diagram

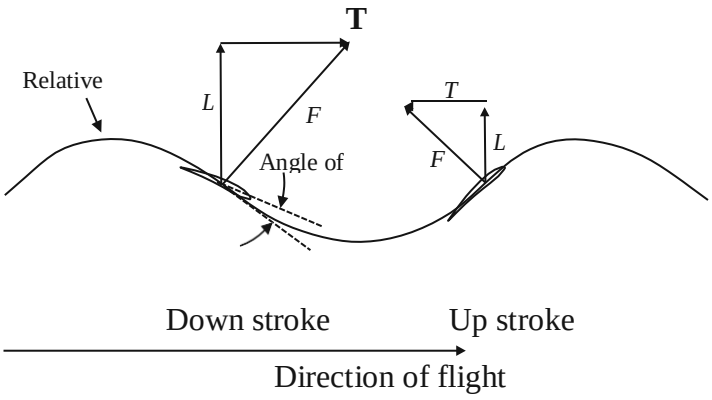

Figure 3.18 Flight of a bird

The direction of the relative wind is tangent to the curved line that varies over the up and down strokes. To maximize the average lift and thrust, the angle of attack is "selected" by the bird to be large during the down stroke, which creates a large net aerodynamic force. This results in a large lift and large positive thrust. During the up stroke, the angle of attack is reduced, leading to a smaller net aerodynamic force. This means that even though the thrust is now negative, the average thrust over a complete cycle is positive. The lift remains positive, although smaller than during the up stroke.

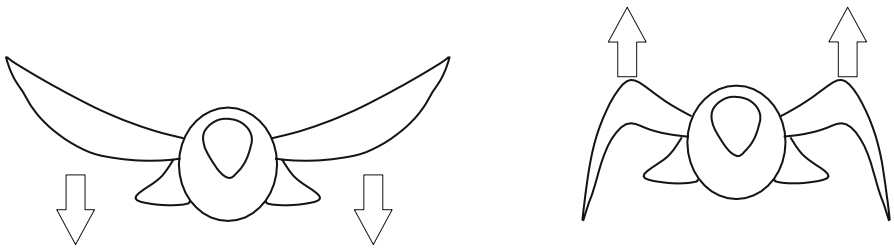

Figure 3.19 Wing articulation

The bird can make the negative thrust during the up stroke even smaller by bending its wings during the up stroke as shown in Figure 3.19. This largely eliminates the forces induced by the outer portions of the wings, which are the most important contributors to thrust, while preserving much of the lift produced near the wing roots.

Total Air-Vehicle Drag

The total resistance to the motion of an air-vehicle wing is made up of two components: the drag due to lift (induced drag), and the profile drag, which in turn is composed of the friction drag and the pressure drag. For the overall air vehicle, the drag of all the non-wing parts are lumped together and called parasite (or parasitic) drag. If the various drag components are expressed in terms of drag coefficients, then simply multiplying their sum by the dynamic pressure q and a characteristic area (usually the wing, S) results in the total drag:

PERFORMANCE

Climbing Flight

An airplane in steady, linear flight is in equilibrium with all the forces acting on it as shown in Figure 4.1. The equations of motion for this condition can be written as:

$$\text{Lift} = W\cos\theta \tag{4.1}$$

where W is weight, and

$$\text{Thrust } (T) = D + W\sin\theta \tag{4.2}$$

where D is drag. Multiplying the second equation by velocity V results in:

$$TV = DV + WV\sin\theta \tag{4.3}$$

where TV is the power delivered to the air vehicle by the propulsion system. It is called power available (PA) and DV is equal to the power required to maintain flight, which is called power required (PR). Since $V\sin\theta$ is equivalent to the rate of climb, dh/dt, the Equation (4.3) can be rewritten as:

$$W\frac{\mathrm{d}h}{\mathrm{d}t} = PA - PR \tag{4.4}$$

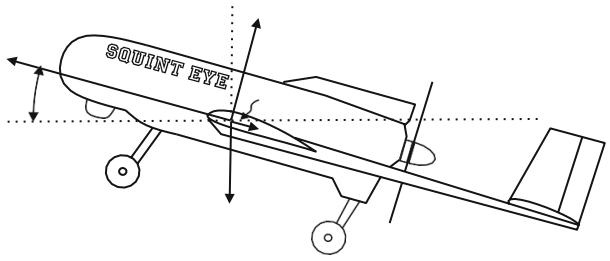

Figure 4.1 Force diagram

Power available can be obtained from the power delivered at the shaft of the engine (P_e) and propeller efficiency (η), expressed as:

$$PA = P_e\eta \tag{4.5}$$

Since PR is equal to drag velocity, our previous discussion of the components of drag as a function of velocity is applicable and both PA and PR can be plotted against velocity as shown in Figure 4.2. From Equation (4.4), the maximum rate of climb takes place at a velocity that has the maximum distance between the two curves. This is also the point where the slopes or derivatives of the two curves are equal. Drag and power are, of course, dependent on air density (among other things) and, therefore, altitude affects both curves.

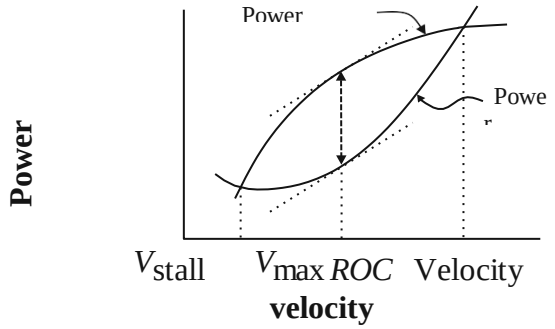

Figure 4.2 Power versus velocity

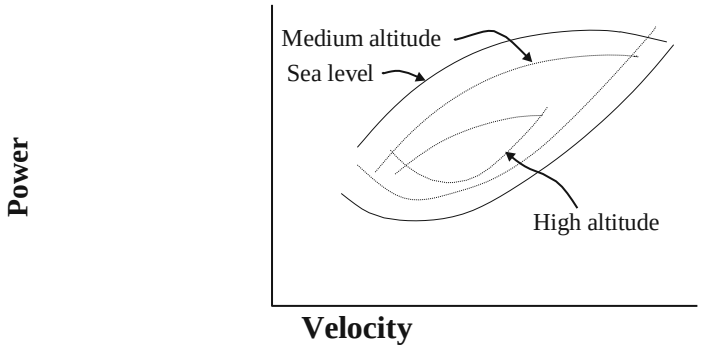

Figure 4.3 Power versus velocity for several altitudes

Figure 4.3 shows typical power-available and power-required curves for several altitudes. One can see that as the altitude increases the distance between the curves, as well as the points where they intersect, become increasingly closer together until the airplane is no longer capable of flight (i.e., there is no place where *PA* is greater than *PR*).Solving Equation (4.4) for d*h*/d*t* (i.e., dividing by *W*), the rate of climb, *ROC*, is easily obtained.

Range

The range of a UAV is an important performance characteristic. It is relatively easy to calculate in a reasonable approximation. The range is dependent on a number of basic aircraft parameters and strongly interacts with the weight of the mission payload, because fuel can be exchanged for payload within limits set by the ability of the air vehicle to operate with varying center of gravity conditions.

The fundamental relationship for calculating range and endurance is the decrease in weight of the air vehicle caused by the consumption of fuel.

For a propeller-driven aircraft, this relationship is expressed in terms of the specific fuel consumption, *c*, which is the rate of fuel consumption per unit of power produced at the engine shaft, P_e. With this definition, we can see that: